Biochemistry

 Volume 19, Number 21 October 14, 1980

Kinetics of Oxidation and Reduction of High-Potential Iron–Sulfur Proteins with Nonphysiological Reactants†

Issac A. Mizrahi,‡ Terrance E. Meyer, and Michael A. Cusanovich*

ABSTRACT: We have investigated the kinetic and equilibrium oxidation–reduction properties of HIPIP's from four sources: *Chromatium vinosum*, *Thiocapsa pfennigii*, *Rhodopseudomonas gelatinosa*, and a *Paracoccus* sp. These studies focused on the interaction of the various HIPIP's and the iron hexacyanides as a function of ionic strength, pH, and temperature. On the basis of the kinetic and equilibrium data obtained and the known structrual properties of the various HIPIP's, a number of conclusions concerning the mechanism of electron transfer by HIPIP can be inferred. (1) The oxidation and reduction of HIPIP by the iron hexacyanides show no kinetic complexity due to heterogeneity or changes in rate-limiting step. (2) The kinetic and equilibrium studies (oxidation–reduction potential) are in good agreement, although a rapid binding equilibrium between HIPIP and the iron hexacyanides is possible. (3) The kinetics of oxidation and reduction of the various HIPIP's studied do not correlate with their oxidation–reduction potentials. (4) The electrostatic interactions between a particular HIPIP and the iron hexacyanides appear to be influenced by the charge on the iron–sulfur cluster with specific amino acid side chains playing a significant but limited role in the interactions leading to electron transfer. (5) The iron–sulfur cluster charge is apparently distributed on the surface of the HIPIP molecule through a network of hydrogen bonds. (6) On the basis of an analysis of the known primary and tertiary structure of the HIPIP's studied, it is concluded that peptide backbone carbonyls and amino acid side chains for the amino acid sequence positions 46–49, 63–65, 78–82, 31–34, and 16–17 define the interaction site of HIPIP and the iron hexacyanides irrespective of the HIPIP source. This is a structural region at which the iron–sulfur cluster is near to the protein surface and in this respect resembles the active site in mitochondrial cytochrome *c*.

The HIPIP[1] class of four-iron, four-sulfur ferredoxins has been established on the basis of apparent amino acid sequence homology among examples from four purple photosynthetic bacteria and a halophilic denitrifying coccus (Dus et al., 1973; Tedro et al., 1974, 1976, 1977). This class of proteins has been extensively investigated, and the three-dimensional structure of one example, from *Chromatium vinosum*, has been determined (Carter et al., 1974a,b). Further, it has been established that the HIPIP class and the low oxidation–reduction potential *Clostridial* ferredoxins contain a common prosthetic group (Carter et al., 1972, 1974a; Freer et al., 1975): a cubane-like complex containing four atoms each of iron and inorganic sulfur bound to the protein via four cysteinyl sulfur ligands. A major distinction between bacterial ferredoxins and HIPIP's is their oxidation–reduction potential, with bacterial ferredoxins having potentials in the vicinity of −400 mV and HIPIP's having potentials near +350 mV. In terms of the iron oxidation–reduction state, the differences in oxidation–reduction potential have been explained on the basis of a "three-state" hypothesis (Carter et al., 1972, 1974a) which proposes that reduced HIPIP and oxidized ferredoxin share a common electron distribution with the protein moiety, preventing further oxidation of ferredoxin or further reduction of HIPIP. The common redox state termed C can be formally represented as $2Fe^{3+}2Fe^{2+}$, with oxidized HIPIP containing $3Fe^{3+}Fe^{2+}$ and reduced ferredoxin having $Fe^{3+}3Fe^{2+}$ (Holm, 1974). The nature of the specific interactions between the protein moiety and the iron–sulfur cluster which leads to the possible redox states is not known in detail. However, Carter (1977) has recently proposed that interactions between the polypeptide backbone and tyrosine side chains in *Chromatium* HIPIP and *Clostridium* ferredoxin place the iron–sulfur clusters of these two proteins into diastereomeric environments, leading to the observed differences in properties.

† From the Department of Biochemistry, University of Arizona, Tucson, Arizona 85721 (I.A.M. and M.A.C.), and the Department of Chemistry, Unviersity of California at San Diego, La Jolla, California 92092 (T.E.M.). *Received January 4, 1980.* This work was supported by research grants from the National Science Foundation (BMS-75-13608 and PCM-7804349) and the National Institutes of Health (GM-18528) and a RCDA from the National Institutes of Health to M.A.C. (KO4EY0013).

‡ Present address: Department of Pathology, University of California at San Diego, La Jolla, CA 92093.

[1] Abbreviation used: HIPIP is an acronym for high-potential iron–sulfur protein. HIPIP is now officially recognized as a high oxidation–reduction potential four iron–sulfur ferredoxin but will be referred to by its trivial name throughout this paper for the sake of brevity and continuity with the literature.

0006-2960/80/0419-4727$01.00/0

The kinetic mechanism by which HIPIP and other ferredoxins undergo oxidation and reduction is poorly understood. Recently we have reported on the reaction of *C. vinosum* HIPIP with a variety of oxidants and reductants (Mizrahi et al., 1976). These studies suggested that HIPIP undergoes outer-sphere electron transfer, with electrostatic interactions playing a role in the rate constants for electron transfer. Further, the reaction of HIPIP with the iron hexacyanides was found to be driven entropically; enthalpic terms make only minor contributions to the rate constants. In a similar study, Rawlings et al. (1976) obtained results for the oxidation and reduction of HIPIP much like those discussed above, although they propose that HIPIP–$Co(phen)_3^{3+}$ and HIPIP–iron hexacyanides employ different mechanisms of electron transfer.

In an effort to obtain a better understanding of the HIPIP class of proteins, we have extended our previous work to include examples of HIPIP from *Rhodopseudomonas gelatinosa*, *Thiocapsa pfennigii*, and a halophilic *Paracoccus* sp. In all cases, the amino acid sequences are known. The studies reported here have focused on the interaction of the iron hexacyanides and the various HIPIP's, with emphasis on the effect of ionic strength and pH on the rate constants of oxidation and reduction and on the oxidation–reduction potential.

Materials and Methods

HIPIP's from *C. vinosum*, *Paracoccus* sp., *T. pfennigii*, and *Rps. gelatinosa* were prepared as described by Bartsch (1978). Stock solutions of the oxidized or reduced proteins were prepared by the addition of a slight excess of potassium ferricyanide or sodium dithionite (Hardman and Holden Limited), and the excess reagent was removed by gel filtration on Sephadex G-25. Studies over a range of pH values were performed in Tris–sodium acetate–glycine–potassium phosphate buffer (TAGP buffer), 25 mM in each component. All chemicals were reagent grade and were used without further purification.

Kinetic studies were conducted in a Durrum-Gibson stopped-flow spectrophotometer with a mixing time of 3 ms. All reactions were maintained at 20 ± 0.2 °C unless otherwise noted. The reaction of reduced HIPIP with potassium ferricyanide was monitored at 500 nm to prevent any interference by the ferricyanide absorbance at 423 nm. Anaeorbic studies were performed as previously described (Miller & Cusanovich, 1975).

Oxidation–reduction potentials were determined by using potassium ferrocyanide–ferricyanide mixtures (Mizrahi et al., 1976). The midpoint potentials for ferri–ferrocyanide given by O'Reilly (1973) were used. All absorption spectra were obtained on a Cary 118 recording spectrophotometer. The equilibrium constant for the dissociation of $S_2O_4^{2-}$ was measured by electron spin resonance as described by Miller & Cusanovich (1975).

For data analysis, we used the integrated rate expression for a reversible first- (pseudo-first-order conditions were maintained) and second-order reaction (A ⇄ B + C), as given by Frost & Pearson (1961), substituting the various absorbance changes (ΔA) for the concentration terms. Equation 1 gives

$$\ln [[\Delta A_t(\Delta A_e - \Delta A_0) + \Delta A_e(2\Delta A_0 - \Delta A_e)]/(\Delta A_t \Delta A_0)] = k_{obsd}[(2\Delta A_0 - \Delta A_e)t/\Delta A_e] \quad (1)$$

the expression used: k_{obsd} is the second-order rate constant (k_{12} for reduction; k_{43} for oxidation) times the reductant or oxidant concentration; ΔA_t is the absorbance change at any time t; ΔA_0 is the total absorbance change that would be observed if the reaction were to go to completion; ΔA_e is the maximum observed absorbance change for the particular oxidant or reductant concentration. If eq 1 is not used, the second-order plots (k_{obsd} vs. [reactant]) deviate from linearity at low reactant concentrations. The observed ΔA_t values were fitted to eq 1 with a Data General Nova II computer to obtain k_{obsd} at any oxidant or reductant concentration. The value ΔA_0 for a particular experiment was calculated from the HIPIP concentration by using the following molar difference extinction coefficients: *C. vinosum* HIPIP, $\Delta E_{480nm} = 8270$ and $\Delta E_{500nm} = 7890$; *Rps. gelatinosa* HIPIP, $\Delta E_{480nm} = 8940$ and $\Delta E_{500nm} = 8470$; *T. pfennigii* and *Paracoccus* sp. HIPIP, $\Delta E_{480nm} = 8510$ and $\Delta E_{500nm} = 8300$.

For all the reactions reported here, the ΔA_t vs. time relation appears accurately first order in terms of eq 1 for at least three half-lives. Further, plots of k_{obsd} vs. reactant were linear in all cases for the concentration range studied, usually 20 μM–10 mM oxidant or reductant, with the HIPIP concentration 5–10 μM.

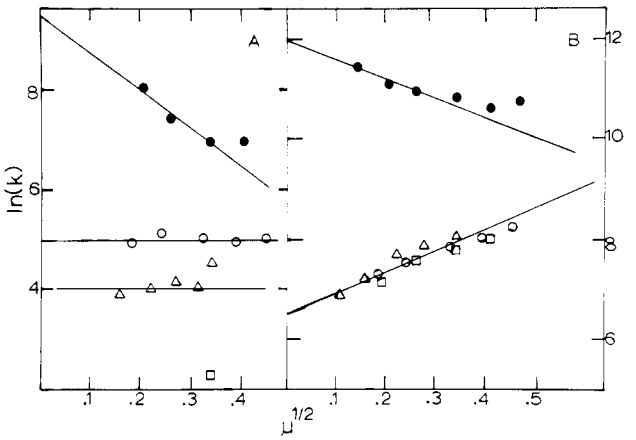

FIGURE 1: Effect of ionic strength on the oxidation and reduction kinetics of HIPIP. (●) *Rps. gelatinosa*; (○) *Chromatium*; (△) *Thiocapsa*; (□) *Paracoccus*. (A) Reduction by potassium ferrocyanide; buffer was 20 mM potassium phosphate, pH 7.0, supplemented with NaCl to give the appropriate ionic strength, 20 °C. Plotted is the observed second-order rate constant at any ionic strength against the square root of the ionic strength (μ). (B) Oxidation by potassium ferricyanide; conditions were as in part A.

Results

Effect of Ionic Strength. The second-order rate constant for reduction of *Rps. gelatinosa* HIPIP by potassium ferrocyanide decreased with increasing ionic strength which is consistent with the ferrocyanide anion reacting with a positively charged HIPIP. Both *Chromatium* and *Thiocapsa* HIPIP have rate constants independent of ionic strength on reduction (μ = ~20–120 mM) which is consistent in both cases with the HIPIP having no apparent charge over this ionic strength range. These data are summarized in Figure 1A in which ln (k_{obsd}) is plotted against $\mu^{1/2}$. Reduction of *Paracoccus* HIPIP was studied only at one ionic strength because potassium ferrocyanide is a poor reductant due to the low midpoint potential of this HIPIP (see later sections) and only limited quantities of the protein were available. Oxidation of *Rps. gelatinosa* HIPIP by potassium ferricyanide was rapid, and the rate constant decreased with increasing ionic strength as was found for reduction (Figure 1B). HIPIP's from *Chromatium*, *Thiocapsa*, and *Paracoccus* all have rate constants for oxidation which increase slightly with increasing ionic strength, consistent with the protein being negatively charged over the ionic strength range studied (Figure 1B). Within experimental error, *Chromatium*, *Thiocapsa*, and *Paracoccus* HIPIP all have rate constants with identical ionic strength dependencies.

Table I: Kinetics of Oxidation and Reduction of HIPIP

HIPIP source	μ[a]	HIPIP redn, k_{12} (M^{-1} s^{-1})	HIPIP oxidn, k_{43} (M^{-1} s^{-1})	K_{eq} (kinetic)	K_{eq} (redox)
Rps. gelatinosa	0.12	1×10^3	5.3×10^4	0.02	0.03[b]
Chromatium[c]	0.11	152	2.5×10^3	0.06	0.11[d]
Thiocapsa	0.08	63	2.8×10^3	0.02	0.08[e]
Paracoccus	0.12	9	2.3×10^3	0.004	0.01[f]

[a] Buffer: 20 mM potassium phosphate, pH 7.0, supplemented with NaCl. [b] μ = 0.29 M; 25 mM TAGP supplemented with NaCl to give the indicated ionic strength, 25 °C. [c] Data from Mizrahi et al. (1976). [d] μ = 0.09 M; 25 mM TAGP supplemented with NaCl, 25 °C. [e] μ = 0.12 M; 25 mM TAGP supplemented with NaCl, 25 °C. [f] μ = 0.02 M; TAGP concentration was adjusted to give indicated ionic strength, 25 °C.

Table II: Effect of Temperature on HIPIP Oxidation and Reduction[a]

	redn			oxidn		
HIPIP source	$\Delta H^{\ddagger}$ (kcal/mol)	$\Delta S^{\ddagger}$ (eu)	$\Delta G^{\ddagger}$ (kcal/mol)	$\Delta H^{\ddagger}$ (kcal/mol)	$\Delta S^{\ddagger}$ (eu)	$\Delta G^{\ddagger}$ (kcal/mol)
Rps. gelatinosa	3.7	−32.7	13.3	0	−40.7	11.9
C. vinosum[b]	4.2	−34.8	14.4	0	−45.1	13.2

[a] Buffer: 50 mM potassium phosphate, pH 7.0. [b] Data from Mizrahi et al. (1976).

Table I presents typical rate constants for the oxidation and reduction of the various HIPIP's and the equilibrium constant (K_{eq}) for the reaction with the iron hexacyanides as calculated from the kinetic data (k_{12}/k_{43}) and as measured by oxidation–reduction titrations (see later sections). In general, the two values of K_{eq} are in reasonable agreement, remembering that the kinetic and equilibrium experiments were conducted at different temperatures (20 vs. 25 °C) and ionic strengths (see Table I).

Effect of pH. The effect of pH on the kinetics of oxidation and reduction of HIPIP from *Chromatium*, *Rps. gelatinosa*, and *Thiocapsa* is given in Figure 2. For clarity, dashed lines have been drawn through the data but have no quantitative meaning. Due to the lack of stability of HIPIP at pH values below 5 or above 11, only a limited pH range could be studied. The *Chromatium* HIPIP data suggest a pK value below 7 in the oxidized state and below 6 in the reduced states. *Thiocapsa* HIPIP resembles *Chromatium* HIPIP in appearing to have a pK below 7 in both redox states, but the effect of pH on the rate of reaction is much more dramatic. Unfortunately, the limited pH range available is not sufficient to specify the pK values. In contrast, the *Rps. gelatinosa* HIPIP data (Figure 2) can be fit with pK values of 7.3 (oxidized) and 7.8 (reduced).

Effect of Temperature. The various thermodynamic activation parameters determined for *Chromatium* and *Rps. gelatinosa* HIPIP's from the effect of temperature on the kinetics of oxidation and reduction are given in Table II. The similarity of the enthalpic and entropic terms for the two HIPIP's is striking. In both cases oxidation has only an entropic term and reduction is primarily entropic with $\Delta H^{\ddagger}$ contributing only 25–30% of the total free energy of activation.

Reduction by Sodium Dithionite. Previous studies established that sodium dithionite reduced *C. vinosum* HIPIP in a kinetically complex fashion; both SO_2^- ($k = 2.1 \times 10^6$ M^{-1} s^{-1}) and $S_2O_4^{2-}$ ($k = 1.2 \times 10^3$ M^{-1} s^{-1}) were reactive, and ionic strength had no influence on the reaction as found for ferrocyanide reduction (Mizrahi et al., 1976). To extend our analysis, we have investigated the reduction of *Rps. gelatinosa* HIPIP by sodium dithionite at three ionic strengths. These data, summarized in Table III, demonstrate that both $S_2O_4^{2-}$ and SO_2^- are active reductants of *Rps. gelatinosa* HIPIP and are consistent with the results obtained with potassium ferrocyanide in which the rate constant decreases with increasing ionic strength, indicating a plus–minus interaction.

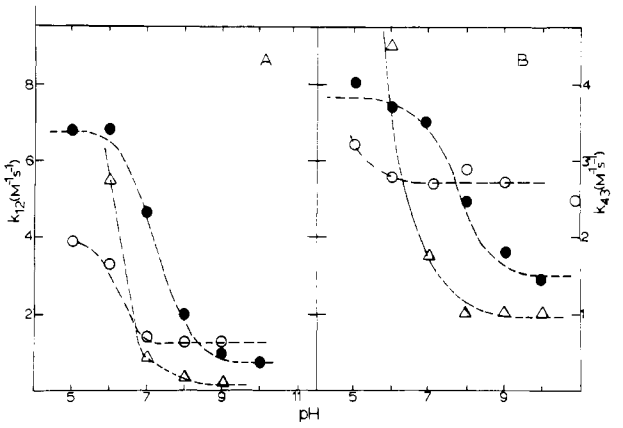

FIGURE 2: Effect of pH on the oxidation and reduction kinetics of HIPIP. (●) *Rps. gelationsa*; (○) *Chromatium*; (△) *Thiocapsa*. (A) Reduction by potassium ferrocyanide; buffer was 25 mM TAGP, 20 °C. The dashed lines were hand drawn for clarity. For *Chromatium* and *Thiocapsa* HIPIP, the ordinate is times 10^{-2}; for *Rps. gelatinosa* HIPIP, the ordinate is times 10^{-3}. (B) Oxidation by potassium ferricyanide. Conditions as in part A. For *Chromatium* and *Thiocapsa* HIPIP, the ordinate is times 10^{-3}, and it is times 10^{-4} for *Rps. gelatinosa* HIPIP.

Table III: Effect of Ionic Strength on the Reduction of *Rps. gelatinosa* HIPIP by Sodium Dithionite[a]

μ (M)	$k_{S_2O_4^{2-}} \times 10^{-3}$ (M^{-1} s^{-1})	$k_{SO_2^-} \times 10^{-6}$ (M^{-1} s^{-1})
0.05	2.0	9.4
0.10	1.6	6.6
0.15	1.2	3.5

[a] Buffer: 10 mM potassium phosphate, pH 7.0, supplemented with the appropriate amount of NaCl to give the indicated ionic strength, 20 °C; [HIPIP] ≃ 10 μM.

Oxidation–Reduction Potentials. Table IV summarizes the effect of pH on the oxidation-reduction potential of HIPIP from *Rps. gelatinosa*, *Chromatium*, *Thiocapsa*, and *Paracoccus*. Figure 3 presents these data graphically. The dashed lines were hand drawn for clarity. *Chromatium* HIPIP has no apparent ionizations that influence the oxidation–reduction potential between pH 7 and pH 11, a result similar to that obtained from an analysis of the effect of pH on the kinetics of oxidation and reduction (Figure 2). The effect of pH on the oxidation–reduction potentials of *Paracoccus*, *Rps. gelatinosa*, and *Thiocapsa* HIPIP suggests that ionizations with

Table IV: Effect of pH on the Oxidation-Reduction Potential of HIPIP[a]

HIPIP source pH	E_m (mV) *Chromatium*[b]	*Rps. gelatinosa*[c]	*Thiocapsa*[d]	*Paracoccus*[e]
5.0	387		376	299
5.2		355		
5.5			367	
6.0	372	345	354	292
6.5			353	
6.6		336		
7.0	356	332	352	282
7.5			347	
8.0	358		339	280
8.1		327		
9.0	355	313	329	268
10.0	358	312	329	255
11.0	352			

[a] Buffer: 25 mM TAGP supplemented with NaCl (except *Paracoccus* HIPIP), 25 ± 1 °C; [HIPIP] ≃5 μM. [b] μ = 0.14 M. [c] μ = 0.29 M. [d] μ = 0.12 M. [e] μ = 0.02 M; TAGP concentration was adjusted to give indicated ionic strength.

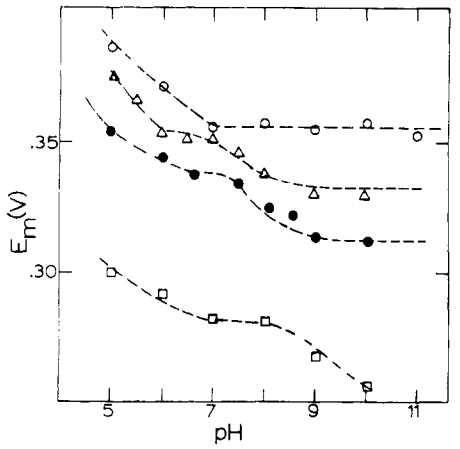

FIGURE 3: HIPIP oxidation–reduction potentials. (○) *Chromatium* HIPIP; (●) *Rps. gelatinosa* HIPIP; (△) *Thiocapsa* HIPIP; (□) *Paracoccus* HIPIP. Conditions were as given in footnotes to Table IV. The dashed lines were hand drawn for clarity. Redox potentials given are average values of two to four determinations at a particular pH and are accurate to ±3 mV.

pK values greater than 6.0 are involved in each case. No quantitative analysis of the pH effects was attempted because the instability of HIPIP below pH 4 or above pH 10 limited the pH range which could be studied.

Discussion

The kinetics of oxidation and reduction of HIPIP by non-physiological oxidants and reductants are consistent with a simple, reversible process. The measured kinetics show no complexity (due to multiple species or changes in rate-limiting steps) over a wide range of oxidant and reductant concentrations and reactant conditions (pH, ionic strength, and temperature). The ratio of the observed rate constants (k_{43}/k_{12}) yields a K_{eq} for reaction with the iron hexacyanides in reasonable agreement with the K_{eq} determined from the oxidation–reduction potentials of the HIPIP and the iron hexacyanides (Table I). On the basis of these results, we have to conclude that no long-lived intermediates (>2 ms) exist and that the HIPIP–iron hexacyanide reaction behaves as a second-order process. However, such a conclusion does not exclude the possibility that HIPIP and its reactants are in rapid equilibrium with a complex. In this case the apparent second-order rate constant would be the product of the equilibrium constant for complex formation and the limiting first-order rate constant going to products (Cusanovich, 1978). If a rapid equilibrium for binding of reactants exists, then the observed linear second-order plots only put a lower limit on any limiting first-order rate constants. In the cases of HIPIP oxidation and reduction by the iron hexacyanides, these lower limits would be 10–500 s^{-1} and 10–100 s^{-1}, respectively, depending on the particular HIPIP. Although a rapid equilibrium between reactants and a complex likely exists, the available kinetic data are not resolvable in this regard; hence, subsequent discussion will be in terms of the apparent second-order rate constants.

Table V: Properties of HIPIP[a]

HIPIP source	P_I	Asp and Glu	Lys and Arg	His	net charge,[b] pH 7.0	no. of AA
C. vinosum	3.7	10	7	1	−3	85
Rps. gelatinosa	9.5	5	10	1	+5	74
Thiocapsa	acidic	11	4	4	−7	81
Paracoccus	acidic	11	1	2	−10	71

[a] Data from amino acid sequences (Dus et al., 1973; Tedro et al., 1974, 1976, 1977) and Bartsch (1978). [b] Does not include the N- and C-terminus charge or iron-sulfur cluster charge (−1, oxidized; −2, reduced). The pK values of the histidine residues are not known, and histidine was assumed not to be protonated.

Table V summarizes the net charge at pH 7.0 and other properties of the various HIPIP's studied and serves as a starting point for a discussion of the effect of ionic strength on HIPIP oxidation and reduction. The net charge given in Table V does not include the contribution of the iron–sulfur cluster which is presumed to be −1 for oxidized HIPIP and −2 for reduced HIPIP (Holm, 1974). On the basis of the net protein charge and measured isoelectric point, ionic strength would be expected to have opposite effects on the interaction of *Chromatium*, *Thiocapsa*, and *Paracoccus* HIPIP as compared to that of *Rps. gelatinosa* HIPIP. This was true for HIPIP oxidation (Table I) but not true for HIPIP reduction, in which the acidic HIPIP's were found to have rate constants for reduction that were apparently independent of ionic strength. Further, the three acidic HIPIP's had very similar ionic strength dependencies for ferricyanide oxidation which is inconsistent with the large differences in net charge among these HIPIP's. Nevertheless, it is difficult to quantitate the ionic strength effects noted. Koppenol (1980) has recently suggested that the ionic strength dependence for a particular reaction will depend on the dipole moment of the protein, the dipole orientation relative to the reactant and the net protein charge. Thus, the results presented here establish that treatment of the ionic strength data in terms of simple charged species is not adequate and suggest that specific interactions between HIPIP and the iron hexacyanides control electron transfer.

In all cases examined, the apparent charge on reduced HIPIP was more negative than that on the oxidized species independent of the net protein charge. A plausible explanation for this observation is that the iron–sulfur cluster is more negatively charged in the reduced form than in the oxidized form and this difference is seen by an approaching reactant.

Most striking is the observation that the various activation parameters (Table II) are identical for both *Rps. gelatinosa* HIPIP and *Chromatium* HIPIP. These data argue that a similar mechanism is operative in both cases and further support the concept that the net protein charge is not a dominating factor in the reaction mechanism. The previously

reported activation parameters for $Fe(EDTA)_2^{2-}$ reduction of HIPIP are very similar to those reported here (Rawlings et al., 1976). However, $Co(phen)_3^{3+}$ and $Ru(NH_3)_5py^{3+}$ were found to interact with HIPIP by a primarily enthalpic process ($\Delta H^{\ddagger}$, 9–15 kcal/mol) with the entropy of activation only making a minor contribution (7 to −12 eu) (Rawlings et al., 1976; Cummins & Gray, 1977). Gray and co-workers have interpreted these data to mean that very ionic ligands like $EDTA^{2-}$ and CN^- cannot penetrate the protein surface and, hence, do not require "protein activation" which would be driven by enthalpic energy. On the other hand, $Co(phen)_3^{3+}$ and $Ru(NH_3)_5py^{3+}$ have much greater π-donor character and thus could penetrate the protein at a cost of enthalpy (Rawlings et al., 1976; Cummins & Gray, 1977).

The effect of pH on the redox properties of the various HIPIP's is difficult to analyze quantitatively at this time due to the lack of limiting conditions. However, the results presented suggest that a number of ionizations occur in both redox states for a particular HIPIP and that these ionizations affect both the midpoint potential and kinetics of oxidation and reduction. This is particularly striking in the case of *Rps. gelatinosa* HIPIP where p*K* values in the pH range 7–8 for the oxidized and reduced forms are observed. The kinetic results reported as a function of pH are consistent with the view that each of the HIPIP's becomes less negatively charged as the pH is lowered and therefore reacts more readily with the negatively charged iron hexacyanides.

To summarize to this point, the results presented establish that electrostatics play a role in the kinetics of oxidation and reduction of HIPIP but do not appear to correlate with the net protein charge. Importantly, oxidized HIPIP appears more positively charged than reduced HIPIP, suggesting that the charge on the iron–sulfur cluster is observed by the approaching reactant. Finally, no correlation exists between the rate constants for oxidation and reduction and the oxidation–reduction potential (see Tables I and II).

Ideally, the data presented should be interpretable in terms of a consistent model relating the kinetics of the various HIPIP's to their structures. Table VI presents the amino acid sequences of the various HIPIP's. *Chromatium* numbering will be used throughout the following discussion. The dashes in Table VI indicate deletions in the sequences relative to that of *C. vinosum*. Moreover, the amino acid sequence of *Chromatium* HIPIP is different from that published at positions 11, 45, and 74 based on a reevaluation of the amides by the original authors (S. M. Tedro, personal communication). For the discussion which follows, we assume structural similarity in order to analyze the data; that is, except for deletions, we assume that amino acid residues in the same sequence position have the same structural role in the various HIPIP's. In our view, this assumption is justified on the basis of the similarity of the physical–chemical properties of the various HIPIP's and by analogy to the cytochromes *c* where there is extensive structural homology in the absence of appreciable sequence identity (Salemme et al., 1973).

Using the assumptions described above, we have examined the structure of *Chromatium* HIPIP and the related sequence substitutions for other HIPIP's to find structural features which would explain the observed kinetics at any particular ionic strength or range of ionic strength (that is, a positively charged region in *Rps. gelatinosa* HIPIP and an uncharged or slightly negative region on the other HIPIP's). Remembering that the oxidation–reduction kinetics seem to reflect the change in charge on the iron–sulfur cluster, we also attempted to incorporate a means by which the iron–sulfur

Table VI: HIPIP Amino Acid Sequences

	1	10	20	30	40	50
Chromatium	S A P A N A V A A D D A T A I A L K Y N Q D A T K S E R V A A A R P G L P P E E Q H C A N C Q F M Q A D					
Thiocapsa	E D L P H V D A A T N P I A Q S L H Y I E D A N A S E R N P V T K T E L P G S E Q F C H N C S F I Q A D					
Paracoccus	E[a] D L P P L D - P S A E Q A Q A L N Y V K D T A E A A D - H P A H Q E G - - - E Q - C D N C M F F Q A D					
Rps. gelatinosa	- - - A P V D - E K N P Q A V A L G Y V S D A A K A D K - A K Y K Q F V A G S - - H C G N C A L F Q G K					

	60	70	80
Chromatium	A A G A T D E W K G C C Q L F P G K L I N V D G W C A S W T L K A G		
Thiocapsa	- - - - S G A W R P C T L Y P G Y T V S E D G W C L S W A H K T A		
Paracoccus	- - - - - - S Q G C C Q L F P Q N S V E P A G W C Q S W T A Q N -		
Rps. gelatinosa	- - - A T D A V G G C C P L F A G K Q V A N K G W C S A W A K K A -		

[a] Glutamine pyrrolidone.

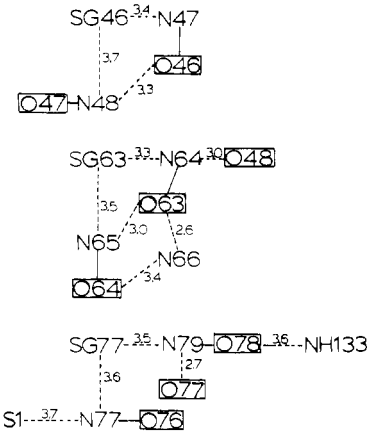

FIGURE 4: Distribution of iron–sulfur cluster charge via hydrogen-bonded networks. The distance between the γ-sulfur of cysteine residues 46, 63, and 77 and nearest neighbors was calculated from the *C. vinosum* HIPIP coordinates. The dashed lines represent probable hydrogen bonds with the calculated distances given in the figure. Solid lines are between peptide amides and their coupled carbonyls. Boxes are drawn about carbonyl oxygens where the delocalized charge would likely reside.

cluster charge could be transferred to the protein surface and interact with the approaching reactant. Carter et al. (1974a) have reported that three of the cysteine sulfurs and one inorganic sulfur bonded to iron appear to be within reasonable hydrogen-bond distances of peptide backbone amide hydrogens (3–4 Å). These were cysteine sulfurs 46, 33, and 77 which are hydrogen bonded to amide hydrogens of residues 48, 65, and 79 and inorganic sulfur 1 which is within 3.6 Å of the amide hydrogen of residue 77. To extend these observations, we identified the nearest neighbors of the individual amides mentioned above and their coupled carbonyls to determine if the iron–sulfur cluster charge could be delocalized since it is clear that an iron–sulfur cluster with a formal charge of −2 or −1 would not be stable buried in a hydrophobic pocket (Carter et al., 1974a). Figure 4 presents the results of our nearest-neighbor analysis outlined above with distances determined from the coordinates given in the figure. This analysis indicates that the charge on the iron–sulfur cluster could be delocalized on the carbonyl oxygens of residues 46, 47, 48, 63, 76, 77, and 78 and at least to some extent neutralized by solvent and Arg-33 which was found to have a guanidinium group in this region. An example of delocalization could be protonation of a sulfur atom by an amide proton with the formation of a carboxamide anion which would be resonance stabilized to give a carbonyl oxygen with a partial negative charge. Figure 5 shows a view of the four HIPIP's studied in the region of the carbonyl oxygens indicated above. It is most striking that of the eight carbonyls coupled to the cysteinyl and inorganic sulfurs, six (excluding 76 and 77) would be encountered by a reactant approaching in the region shown in Figure 5. Further, it can be seen that the amino acid side chains most proximal to an approaching reactant would be 46–49, 63–65, and 78–82 with the side chains of residues 31–34 and 16–17 nearby. Carter et al. (1974a) pointed out that solvent access to the iron–sulfur cluster is most likely in the region of inorganic sulfur atoms S2 or S4 (see Figure 5) which are only 4.5 Å from the surface of the molecule in the region where the iron–sulfur cluster charge is delocalized. Thus, the analysis presented provides a plausible explanation for the observed kinetics. With the acidic HIPIP's, the reduced iron–sulfur cluster provides a −2 formal charge which is distributed over the carbonyls at position 46–48, 63, 64, and 76–78 and is partially neutralized by a positive charge at

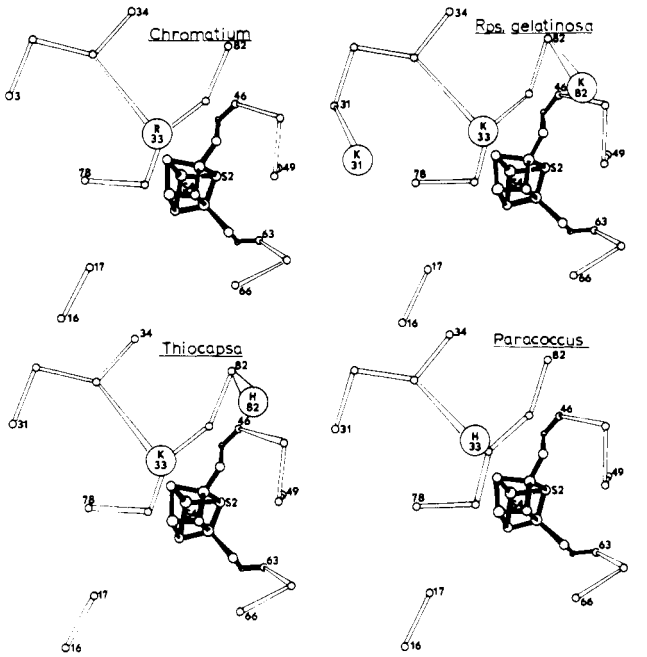

FIGURE 5: HIPIP as viewed in the region of the delocalized charge. All drawings were derived from the coordinates for *Chromatium* HIPIP (Brookhaven Protein Data Bank) with substitutions and deletions inserted in other HIPIP's assuming structural homology.

position 33: arginine (*Chromatium*), histidine (*Thiocapsa* and *Paracoccus*), or lysine (*Thiocapsa*). On oxidation, the formal charge on the iron–sulfur cluster is reduced to −1 and appears uncharged when delocalized and neutralized. On the other hand, *Rps. gelatinosa* HIPIP has three positively charged side chains (positions 31, 33, and 82) in the region of the carbonyls noted above and, hence, has an apparent net positive charge, but that charge is decreased on reduction to a less positive value. In all cases, the approaching reactant would interact in a region where the chromophore is close to the molecular surface.

In summary, the data and analysis presented suggest that electron transfer to and from the iron–sulfur cluster of HIPIP takes place in the region bounded by amino acid side chains 78–81, 47–48, 64–65, and, at a greater distance, 31–34 and 16–17. Although our analysis is only qualitative at this time, it is consistent with available kinetic and structural data. Our focus in the discussion here has been on electrostatic interactions; clearly, other parameters may be involved, including nonpolar interactions and possibly conformational changes. However, an understanding of the relative contribution of interactions other than electrostatic will have to await future studies.

References

Bartsch, R. G. (1978) *Methods Enzymol. 53B*, 329.

Carter, C. W. (1977) *J. Biol. Chem. 252*, 7802.

Carter, C. W., Kraut, J., Freer, S. T., Alden, R. A., Sieker, L. C., Adman, E., & Jensen, L. H. (1972) *Proc. Natl. Acad. Sci. U.S.A. 69*, 3526.

Carter, C. W., Kraut, J., Freer, S. T., & Alden, R. A. (1974a) *J. Biol. Chem. 249*, 6339.

Carter, C. W., Kraut, J., Freer, S. T., Xuong, N. H., Alden, R. A., & Bartsch, R. G. (1974b) *J. Biol. Chem. 249*, 4212.

Cummins, D., & Gray, H. B. (1977) *J. Am. Chem. Soc. 99*, 5158.

Cusanovich, M. A. (1978) in *Frontiers of Biological Energetics* (Leigh, J., Dutton, P. L., & Scarpa, A., Eds.) pp 91–100, Academic Press, New York.

Dus, K., Tedro, S. M., & Bartsch, R. G. (1973) *J. Biol. Chem. 248*, 7318.
Freer, S. T., Alden, R. A., Carter, C. W., & Kraut, J. (1975) *J. Biol. Chem. 250*, 46.
Frost, A. A., & Pearson, R. G. (1961) *Kinetics and Mechanism*, 2nd ed., Wiley, New York.
Holm, R. H. (1974) *Endeavor 34*, 38.
Koppenol, W. H. (1980) *Biophys. J. 29*, 493.
Miller, W. G., & Cusanovich, M. A. (1975) *Biophys. Struct. Mech. 1*, 97.
Mizrahi, I. A., Wood, F. E., & Cusanovich, M. A. (1976) *Biochemistry 15*, 343.
O'Reilly, J. E. (1973) *Biochim. Biophys. Acta 292*, 509.
Rawlings, J., Wherland, S., & Gray, H. B. (1976) *J. Am. Chem. Soc. 74*, 229.
Salemme, F. R., Kraut, J., & Kamen, M. D. (1973) *J. Biol. Chem. 248*, 7701.
Tedro, S. M., Meyer, T. E., & Kamen, M. D. (1974) *J. Biol. Chem. 249*, 1182.
Tedro, S. M., Meyer, T. E., & Kamen, M. D. (1976) *J. Biol. Chem. 251*, 129.
Tedro, S. M., Meyer, T. E., & Kamen, M. D. (1977) *J. Biol. Chem. 252*, 7826.

Electron Transfer Reactions of High-Potential Iron–Sulfur Proteins and *c*-Type Cytochromes†

Issac A. Mizrahi‡ and Michael A. Cusanovich*

ABSTRACT: Studies of electron transfer by biological oxidation–reduction proteins frequently focus on the interaction of a particular protein with nonphysiological oxidants and/or reductants. This approach, although valuable, is limited by the size and chemistry of the nonphysiological reactants. To further the understanding of biological electron transfer, we have investigated the interaction of two examples of high-potential iron–sulfur proteins (HIPIP's) with mitochondrial cytochrome *c* (horse heart) and bacterial cytochrome c_2 from *Rhodospirillum rubrum*, *Rhodopseudomonas palustris*, *Rhodopseudomonas capsulata*, and *Rhodopseudomonas sphaeroides*. On the basis of the kinetics of electron transfer between the various HIPIP's and cytochromes, it appears that the interactions are more complex than those observed with nonphysiological reactants. We conclude that (1) specific sites on both the HIPIP's and the cytochromes mediate electron transfer with the effect of ionic strength different from that expected on the basis of the interaction of the various proteins with the iron hexacyanides, (2) the interaction of HIPIP with some of the cytochromes investigated is heterogeneous, resulting from at least two possible orientations (cytochrome dependent) for interaction leading to electron transfer, and (3) no long-lived complexes between the HIPIP's and cytochromes are formed due to rapid equilibrium between the two proteins. This last conclusion suggests that the measured second-order rate constant is in fact the product of the association constant (for any HIPIP and a particular cytochrome) and a first-order rate constant reflecting the rate-limiting step leading to products.

In previous publications we reported on the interaction of a class of high-potential iron–sulfur proteins (HIPIP) with nonphysiological oxidants and reductants (Mizrahi et al., 1976, 1980). These studies indicate that electron transfer to the HIPIP iron–sulfur cluster takes place at a specific region on the protein surface and involves electrostatic interactions. Further, it appears that the iron–sulfur cluster charge is distributed on the protein surface in the region of the site of electron transfer (Mizrahi et al., 1980) and affects the kinetics of electron transfer.

The specific electron donor and acceptor that interact with HIPIP in vivo are unclear at the present time although a recent report suggests *Chromatium* HIPIP may serve as an electron acceptor for a thiosulfate oxidizing enzyme (Fukumori & Yamamaka, 1979). In a preliminary communication, we have reported on the interaction of HIPIP with several *c*-type cytochromes (Cusanovich & Mizrahi, 1979). Although no convincing evidence exists that *c*-type cytochromes naturally interact with HIPIP, this reaction provides a particularly useful model system in that substantial structural information concerning both *c*-type cytochromes and HIPIP is available (Carter et al., 1974, Freer et al., 1975; Salemme et al., 1973; Dickerson et al., 1971). Further, many *c*-type cytochromes have oxidation–reduction potentials similar to HIPIP, thus providing kinetic data on both oxidation and reduction. Our previous studies with *c*-type cytochromes suggested that neither the oxidation–reduction potential nor the structure of the cytochromes in the region of the exposed heme edge (the supposed site of electron transfer) played a measurable role in the reaction with HIPIP (Cusanovich & Mizrahi, 1979). In addition, contrary to the conclusions with nonphysiological reactants, electrostatic interactions were not thought to be of major importance over the ionic strength range studied. We report here more extensive studies on the interaction of HIPIP from two sources (*Chromatium vinosum* and *Rhodopseudomonas gelatinosa*) with horse heart cytochrome *c* and cytochrome c_2 from *Rhodospirillum rubrum*, *Rhodopseudomonas capsulata*, and *Rhodopseudomonas palustris*.

Materials and Methods

HIPIP's from *C. vinosum* and *Rps. gelatinosa* were prepared as described previously (Cusanovich, 1967; Bartsch,

† From the Department of Biochemistry, University of Arizona, Tucson, Arizona 85721. *Received January 4, 1980.* This work was supported by research grants from the National Science Foundation (PCM 7804349) and the National Institutes of Health (GM 21277) and a RCDA from the National Institutes of Health to M.A.C. (KO4EY0013).

‡ Present address: Department of Pathology, University of California at San Diego, La Jolla, CA 92093.

0006-2960/80/0419-4733$01.00/0